

Original Article

Upregulation of SPI1 during myocardial infarction aggravates cardiac tissue injury and disease progression through activation of the TLR4/NFκB axis

Zhengling Liu¹, Shuai Huang²

¹Department of Cardiology of Traditional Chinese Medicine, Dongying Hospital of Traditional Chinese Medicine, Dongying 257055, Shandong, P. R. China; ²Department of Cardiovascular Medicine, Panjin Liaohe Oil Gem Flower Hospital, Panjin 124010, Liaoning, P. R. China

Received January 14, 2022; Accepted March 21, 2022; Epub April 15, 2022; Published April 30, 2022

Abstract: Objective: Spleen focus forming virus proviral integration oncogene (SPI1) belongs to the ETS family of transcription factors participating in an array of cellular processes such as inflammation and cell apoptosis. This research focused on the role of SPI1 in the myocardial infarction (MI). Methods: A murine model of MI was established. HL-1 cells were exposed to hypoxic treatment to simulate an MI-like condition. Tissue injury, inflammatory infiltration, and fibrosis in the cardiac tissues, and the apoptosis and the production of inflammation-related factors in cells were examined. Expression of SPI1 was determined. The downstream targets of SPI1 were identified by bioinformatics tools and luciferase assays. Artificial up- or downregulation of SPI1 and toll like receptor 4 (TLR4) were induced to examine their involvements in MI progression. Results: SPI1 was expressed at high levels in the cardiac tissues of MI mice and in hypoxia-induced HL-1 cells. SPI1 downregulation reduced apoptosis and the production of inflammatory cytokines in the hypoxia-induced HL-1 cells. SPI1 bound to TLR4 promoter to induce transcriptional activation. TLR4 induced NFκB phosphorylation and blocked the protective role of SPI1 silencing in cells. *In vivo*, SPI1 inhibition restored the cardiac function and ameliorated MI-induced inflammation and fibrosis in mice. The protective role of SPI1 inhibition in mice was blocked by TLR4 activation. Aberrant upregulation of SPI1 was caused by the reduced DNA methylation during MI. Conclusion: This study demonstrated that upregulation of SPI1, caused by reduced DNA methylation, augmented development of myocardial infarction by activating the TLR4/NFκB axis.

Keywords: Myocardial infarction, DNA methylation, Spi-1 proto-oncogene, toll like receptor 4, nuclear factor kappa B

Introduction

Myocardial infarction (MI) is a heart attack caused by the formation of plaque or buildup of fatty materials in the arterial interior walls. It leads to a reduction of blood flow to the heart and a consequent cardiac injury because of a lack of oxygen supply [1]. The major presentations of MI are chest pain, sweating, abnormal heart beat, shortness of breath, nausea, anxiety, and fatigue [2]. Although the evolving understanding of MI pathogenesis and the new treatment strategies, including immediate reperfusion and guideline-directed medical therapies, have significantly improved survival rates of patients, there remain major challenges in MI management. Patients with cardiogen-

ic shock have an over 40% mortality within 30 days [3]. During MI, buildup left ventricular mass and progressive myocardial thickening are major characteristics of cardiac remodeling which leads to cardiac hypertrophy, fibrosis, and apoptosis [4]. Cardiomyocyte apoptosis in the ischemia area enlarges the infarct size and induces an inflammatory response and the subsequent cardiac injury and remodeling [5]. Developing more effective strategies to prevent cardiomyocyte loss may help improve the survival of patients.

Spleen focus forming virus proviral integration oncogene (SPI1, also termed PU.1) belongs to the ETS family of transcription factors that participate in cellular processes, such as prolifera-

SPI1-mediated TLR4 augments cardiac injury in MI

tion, transformation, and immune cell development [6]. SPI1 is closely correlated to myeloid cell development, function, and hematopoiesis [6, 7]. SPI1 has been identified as one of the key factors involved in the development of post-MI heart failure, which was correlated with inflammation, immune activity, and cell apoptosis [8]. The exact function of SPI1 in MI development is not that clear. The bioinformatics analyses in this study predicted toll like receptor 4 (TLR4) as a potential target of SPI1. TLR4 is a member of the TLRs that play critical roles in mediating tissue injury and inflammation in response to inflammatory stimuli [9]. The TLRs are pattern recognition receptors frequently implicated in cardiovascular diseases [10]. TLR4 is a class of innate immune receptors recognizing a multitude of ligands. Its activation upon myocardial ischemia/reperfusion may lead to nuclear translocation and phosphorylation of nuclear factor kappa B (NFκB) [11, 12]. Activation of the TLR4/NFκB has been associated with cardiac inflammation and myocardial apoptosis in mice with acute MI [13]. Whether SPI1 regulates the TLR4/NFκB axis to mediate cardiac tissues attracted our interests. This research was carried out to validate the expression profiling of SPI1 and its role in the development of MI.

Materials and methods

Animal model

Seventy male specific-pathogen-free (SPF) grade C57BL/6J mice (8 weeks old, 21.09 ± 1.12 g) were procured from Vital River Laboratory Animal Technology Co., Ltd. (Beijing, China). All mice were maintained in SPF-grade animal rooms with constant temperature (22°C - 25°C) and humidity (60%-65%). The animals were provided with water and fed freely. The research was ratified by the Animal Ethics Committee of Dongying Hospital of Traditional Chinese Medicine (Approval No. #20201109). All animal experiments were adhered to the Guide for the Care and Use of Laboratory Animals (NIH, Bethesda, Maryland, USA). Significant efforts were made to reduce the suffering of animals.

After acclimation for one week, the mice were randomly assigned into five groups: sham group ($n = 10$), MI group ($n = 15$; model mice with MI), AAV-NC group ($n = 15$; AAC refers to adeno-associated virus and NC to negative

control; mice were injected with AAV-NC prior to MI induction), AAV-siRNA-SPI1 group ($n = 15$; siRNA refers to small interfering RNA; mice were injected with AAV-siRNA-SPI1 prior to MI induction), and AAV-siRNA-SPI1 + AAV-TLR4 group ($n = 15$; mice were injected with AAV-siRNA-SPI1 and AAV-TLR4 prior to MI induction).

The SPI1-suppressive AAV-siRNA-SPI1, the TLR4-overexpressing AAV-TLR4, and the AAV-NC were acquired from GenePharma Co., Ltd. (Shanghai, China). The serotype of AAV is AAV-9 with good affinity for the heart, and the AAV contained the cardiomyocyte-specific promoter cardiac troponin-T. The virus titer was 10^9 TU/mL. The AAVs were injected into the mouse myocardial tissues using an insulin syringe at 5 different sites one week prior to MI induction. After successful injection, the color of injection sites changed from red to white. Each type of AAV was injected at 5 sites at equal distance intervals. The injection dose was $10 \mu\text{L}$ per site.

The mice were starved overnight before MI induction. The mice were anaesthetized with 50 mg/kg pentobarbital sodium (intraperitoneal injection [i.p.]). The chest was exposed, and the left anterior descending (LAD) artery (2 mm below the left atrial junction) was ligated using a 7-0 suture to induce MI in mice. Sham-operated mice only had the chest opened. A minimum of 10 successfully modeled mice were maintained in each group. The end point of the experiment was the 14th day after MI induction [14].

Examination of the cardiac function

On the 14th day after MI induction, the cardiac function of the mice was examined using a Vevo 2100 System (VisualSonics, Toronto, Canada) for animal echocardiography. The left ventricular end-diastolic diameter (LVEDD) and left ventricular end-systolic diameter (LVESD) in at least three consecutive cardiac cycles were examined. The ejection fraction (EF) and fractional shortening (FS) were calculated to evaluate the systolic function of the heart. The calculation formulas were as follows: $\text{EF} (\%) = \frac{[(\text{LVEDD}^3 - \text{LVESD}^3)]}{\text{LVEDD}^3} \times 100$; $\text{FS} (\%) = \frac{[\text{LVEDD} - \text{LVESD}]}{\text{LVEDD}} \times 100$. After the cardiac function detection, the mice were sacrificed with of 150 mg/kg barbiturate (i.p.). The serum and cardiac tissues were collected.

SPI1-mediated TLR4 augments cardiac injury in MI

Histochemical staining

The cardiac tissues from five mice in each group were collected. The tissues were equally cut into six sections in parallel with the coronary sulcus and ligation lines. The sections were incubated in 2% TTC (Sigma-Aldrich, Merck KGaA, Darmstadt, Germany) at 37°C for 15 min and then fixed in 4% paraformaldehyde (PFA) for 24 h before observation. The infarct size (white) and non-infarct size (red) were analyzed by Image-Pro Plus v6.0. The MI rate was calculated as follows: rate = infarct size/total area × 100%.

The heart tissues from the remaining five mice in each group were harvested and fixed in 4% PFA. Dehydrated tissues were embedded in paraffin and prepared as 4- μ m sections. The sections were dewaxed, rehydrated, and then subjected to hematoxylin and eosin (H&E) staining (G1120, Solarbio Science & Technology Co., Ltd., Beijing, China) and Masson's trichrome staining (G1340, Solarbio) in accordance to the manufacturer's instructions. Immunohistochemical (IHC) staining of the tissue sections was performed using the specific primary antibodies to c-caspase-3 (1:400, #9661, Cell Signaling Technologies (CST), Beverly, MA, USA), SPI1 (1:2,500, ab227835, Abcam Inc., Cambridge, MA, USA), TLR4 (1:20, ab13867, Abcam), and p-NF κ B p65 (Ser536) (1:100, AF2006, Affinity Biosciences, Cincinnati, OH, USA) at 4°C for 16 h. This was followed by reaction with goat anti-rabbit IgG (H&L) (HRP) (1:1,000, ab6721, Abcam) at 37°C for 2 h. The color was developed by DAB. Hematoxylin was used for counterstaining of nuclei. The staining was observed under a microscope (Carl Zeiss, Oberkochen, Germany). The pathological change evaluated by H&E staining was scored from two aspects: the degree of cardiomyocyte hypertrophy (0~3) and the degree of inflammatory infiltration (0~3). The final score was the sum of the above two (0~6). The fibrotic area evaluated by Masson's trichrome staining and the IHC-positive rate of related genes were analyzed by Image-Pro Plus v6.0.

Cell culture and transfection

Immortalized mouse HL-1 cardiomyocytes (CL-0605) were acquired from Procell Life Science & Technology Co., Ltd. (Wuhan, Hubei, China). The HL-1 cells were maintained in minimum

essential medium (PM150410, Procell) containing 10% FBS and 1% penicillin/streptomycin at 37°C with 5% CO₂.

SiRNA of SPI1 (si-SPI1; guide: 5'-UUGGUAU-AGCUCUGAAUCGUA-3'; passenger: 5'-CGAUU-CAGAGCUAUACCAACG-3'), DNA overexpressing vector of TLR4 (oe-TLR4), and the NC were procured from GenePharma and transfected into the cells adhering to the protocol of a Lipofectamine 2000 kit (Thermo Fisher Scientific Inc., Waltham, MA, USA). On one day prior to transfection, cells (1×10^5) were cultured into 24-well plates until reaching a 70-90% cell confluence. After that, 0.6 μ g siRNA (1 μ g DNA) and Lipofectamine 2000 was diluted in a serum-free medium. The two dilutions were mixed at a ratio of 1:1 and incubated at 22-25°C for 5 min. The mixture was loaded into cells, and the culture medium was refreshed after 6 h of incubation. After 48 h, the cells were harvested. The transfection efficiency was observed under microscopy (si-SPI1: 81%; si-NC: 78%; oe-NC: 85%; oe-TLR4: 82%). The cells were then harvested for future usage.

A DNA methyltransferase (DNMT) inhibitor 5-Aza-2'-Deoxycytidine (5-Azadc) was procured from Sigma-Aldrich. The HL-1 cells were treated with 2 μ M 5-Azadc and dissolved in DMSO (Sigma-Aldrich) for 48 h to inhibit the DNA methylation level in cells. Cells treated with an equal volume of DMSO were set as controls. The HL-1 cells were exposed to a hypoxic condition *in vitro* to mimic cell injury in the infarcted border zone in permanent coronary occlusion-induced MI *in vivo* [14, 15]. Cells subjected to hypoxic exposure were cultured in a hypoxic condition (1% O₂) for different time durations (12, 24, 36, and 48 h). Cells cultured in a normoxic condition (21% O₂) were set as controls.

Enzyme-linked immunosorbent assay (ELISA)

The production of interleukin-6 (IL-6) and tumor necrosis factor- α (TNF- α) in mouse serum and the cell culture supernatants were examined using an IL-6 ELISA kit (ab222503, Abcam) and a TNF- α ELISA kit (ab208348, Abcam) following the manufacturer's instruction manual.

Reverse transcription-quantitative polymerase chain reaction (RT-qPCR)

Total RNA from the cells or cardiac tissues was isolated using the TRIzol Reagent (Thermo

SPI1-mediated TLR4 augments cardiac injury in MI

Table 1. Primers used for RT-qPCR

Primers	Sequence (5'-3')
SPI1	F: GAGGTGTCTGATGGAGAAGCTG
	R: ACCCACCAGATGCTGTCCCTCA
TLR4	F: AGCTTCTCCAATTTTCAGAACTTC
	R: TGAGAGGTGGTGAAGCCATGC
GAPDH	F: CATCACTGCCACCCAGAAGACTG
	R: ATGCCAGTGAGCTTCCCGTTCAG

Note: RT-qPCR, reverse transcription-quantitative polymerase chain reaction; SPI1, Spleen focus forming virus proviral integration oncogene; TLR4, toll like receptor 4; GAPDH, glyceraldehyde-3-phosphate dehydrogenase.

Fisher Scientific). High-quality RNA was quantified using ultraviolet analysis. Reverse transcription of RNA to cDNA was performed using a gDNA-eraser-attached PrimeScript™ RT kit (Takara Holdings Inc., Kyoto, Japan). The qPCR was conducted using the TB Green® Premix Ex Taq™ (Takara) on a Lightcycler[®] 480 real-time PCR System (Roche Ltd., Basel, Switzerland). The primer information is listed in **Table 1**. GAPDH was used as the endogenous control for mRNA. The gene expression was evaluated by the $2^{-\Delta\Delta CT}$ method.

Western blot analysis

Total protein from tissues or cells were isolated using the RIPA lysis buffer (Beyotime Biotechnology Co., Ltd., Shanghai, China). After a protein concentration examination by a bicinchoninic acid assay kit (Beyotime), an equal amount of protein sample (30 µg) was subjected to SDS-PAGE and loaded onto polyvinylidene fluoride membranes (Millipore Corp., Billerica, MA, USA). The membranes were blocked and hybridized with primary antibodies at 4°C for 16 h and then with HRP-labeled secondary antibody at 25°C for 1 h. The blot bands were developed using the electrochemiluminescence reagent (Beyotime). The signals were analyzed using the Image Lab™ software (NIH). The antibodies are listed in **Table 2**. GAPDH was used as the endogenous control.

Terminal deoxynucleotidyl transferase (TdT)-mediated dUTP nick end labeling (TUNEL)

A one-step TUNEL kit (Beyotime) was used to examine apoptosis of cardiomyocytes. The cells were fixed and then penetrated in 0.3% Triton X-100-supplemented phosphate-buffer-

ed saline (PBS). The cells were stained using the TUNEL reagent (50 µL). The cells with positive staining in the nuclei were apoptotic cells. The positive cells in six random fields of views were counted under a fluorescence microscope (Zeiss). The apoptosis rate was calculated as follows: rate = TUNEL-positive cells/total cells × 100%.

Chromatin immunoprecipitation (ChIP)-qPCR

Approximately 2×10^7 cells were loaded in 15-mL tubes, fixed for 10 min, and then terminated by 2 mL 250 mmol/L glycine. The sample was lysed and centrifuged to collect the precipitates. The precipitates were resuspended in the buffer [1% SDS, 10 mmol/L EDTA (pH 8.0), and 50 nmol/L Tris (pH 8.0)] and subjected to ultrasonic treatment. The sample was centrifuged to discard the debris. The supernatant was diluted five times and reacted with the ChIP-specific antibodies anti-SPI1 (1:20, ab227835, Abcam), anti-DNMT1 (1:50, #MA5-16169, Thermo Fisher Scientific), anti-DNMT3a (1:50, #49768, CST), anti-DNMT3b (1:50, #48488, CST), and IgG (1:50, ab17-2730, Abcam) at 4°C overnight. On the next day, protein G beads (Thermo Fisher Scientific) were added for 4 h of incubation. The magnetic beads were washed in lysis/washing buffer and in cold Tris-EDTA buffer (Thermo Fisher Scientific). The DNA-protein complexes were de-crosslinked, and the DNA molecules were purified and quantified using qPCR.

For tissues, the mouse cardiac tissues were cut into 1-mm³ blocks, which were loaded into 50-mL tubes, added with 10 mL PBS, fixed with formaldehyde (final concentration of 1%), and treated with glycine to terminate cross-linking. The samples were then centrifuged at 100 g at 4°C for 5 min to discard the supernatant. The precipitates were lysed in lysis/washing buffer. After three repetitions of centrifugation at 100 g at 4°C for 5 min, the precipitates were collected. The DNA sample was collected for qPCR as previously described. The sequence information of the ChIP primer is listed as follows: TLR4 promoter: forward primer: 5'-ACTGTGCTCTGGGAGACTTG-3'; reverse primer: 5'-CTGGAGGAACAGCAAGAGGA-3'; SPI1 promoter: forward primer: 5'-ACGGACAGACAAGTGGCTAA-3'; and reverse primer: 5'-AAACCTTCTCGCACGTTTC-3'.

SPI1-mediated TLR4 augments cardiac injury in MI

Table 2. Antibodies for western blot analysis

Antibodies	Dilution	Item. No.	Manufacture
SPI1	1:1,000	ab227835	Abcam
TLR4	1:1,000	#14358	Cell signaling technology
p-NFκB p65 (Ser468)	1:1,000	#3039	Cell signaling technology
NFκB p65	1:1,000	#8242	Cell signaling technology
GAPDH	1:10,000	ab181602	Abcam
IgG H&L (HRP)	1:10,000	ab6721	Abcam

Note: SPI1, Spleen focus forming virus proviral integration oncogene; TLR4, toll like receptor 4; NFκB, nuclear factor kappa B; GAPDH, glyceraldehyde-3-phosphate dehydrogenase; IgG, immunoglobulin G; HRP, horseradish peroxidase.

Luciferase assay

The putative binding site between TLR4 promoter and SPI1 was predicted using Jaspar (<http://jaspar.genereg.net/>). The wild-type (WT) TLR4 promoter sequence containing the binding site with SPI1, or the mutant-type (MT) TLR4 promoter sequence was inserted into the pGL3-Basic (Promega, Madison, WI, USA) to construct luciferase reporter vector, named Promoter-WT and Promoter-MT, respectively. The Promoter was co-transfected with si-NC or si-SPI1 into HL-1 cells by Lipofectamine 2000. The luciferase activity in cells was examined 48 h later adhering to the protocol of the dual luciferase reporter assay kit (Promega).

Quantitative methylation specific PCR (qMSP)

DNA from tissue sections was extracted and isolated by an Ion AmpliSeq™ Direct FFPE DNA Kit (Thermo Fisher Scientific). DNA from cells was extracted using a Cell genomic DNA Extraction Kit (Bio-Lab Technologies, Beijing, China). The DNA purity and concentration were detected using a NanoPhotometer spectrophotometer and Qubit2.0 Fluorometer. An EZ DNA Methylation-Gold kit™ (Zymo Research Corp., Orange, CA, USA) was used for bisulphite treatment. The product was subjected to Sanger sequencing to examine its specificity for qMSP. The methylation level of SPI1 was examined using qPCR. The SPI1-specific primers for qMSP were as follows: MF: 5'-GTTGGTAGTAA-GAAATTATCGGGG-3', MR: 5'-TAACCTAACTATC-ACGAACTCG-3'; UF: 5'-GTTGGTAGTAAGAAAT-TATTGGGG-3', and UR: 5'-ACCTAACTATCACAA-AACTCACTC-3'.

Statistical analysis

All data were presented as the mean ± standard deviation (SD). Data analyzed was performed by the Prism 8.02 (GraphPad, La Jolla,

CA, USA). Differences were compared by the unpaired *t* test (two groups), or by one- or two-way analysis of variance (ANOVA) followed by Tukey's multiple test (over two groups). *P* < 0.05 was set to the threshold value for significant difference.

Results

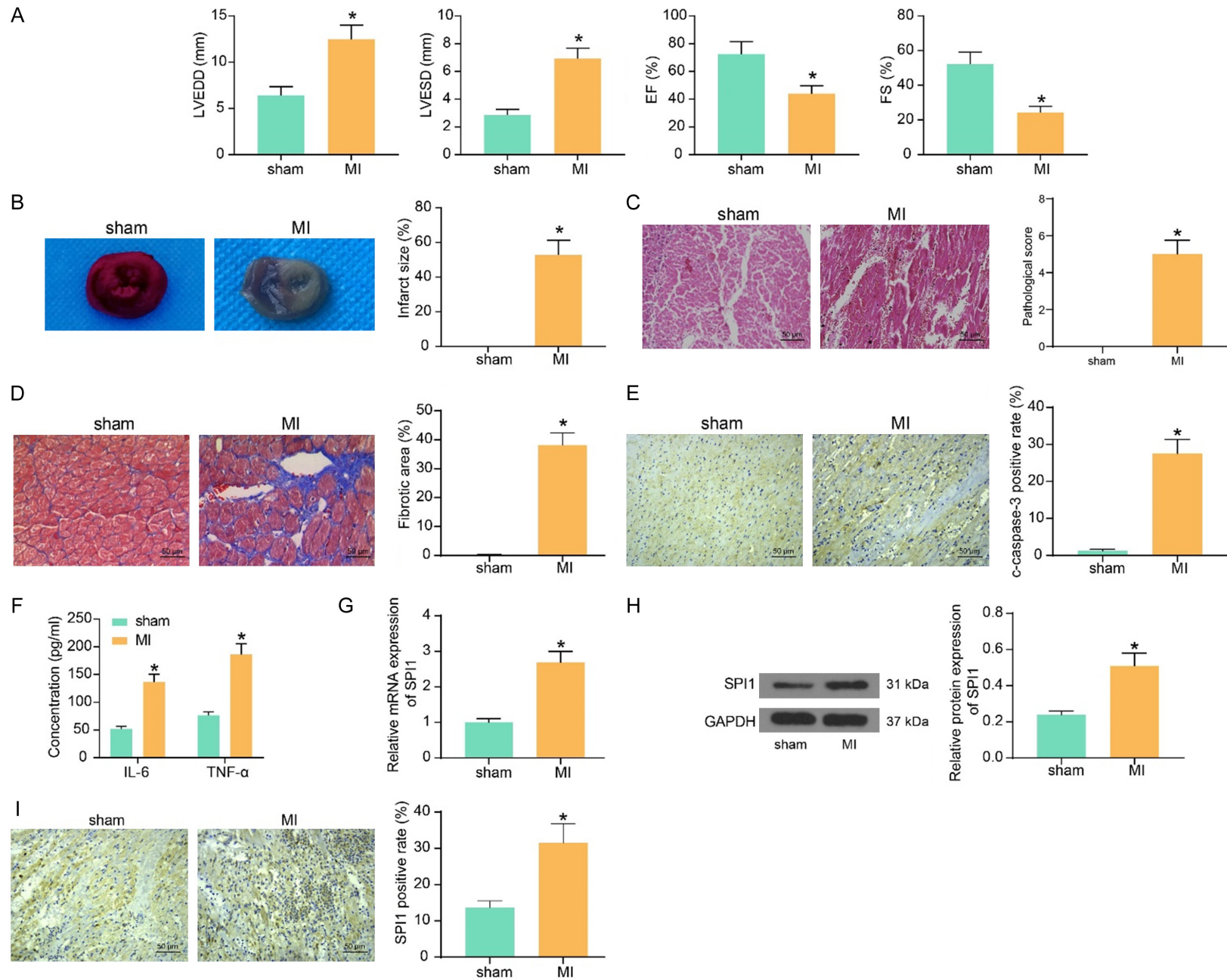
SPI1 expression was increased in cardiac tissues of model mice

A murine model of MI was induced by LAD artery ligation, and the sham-operated mice only had the chest opened. The cardiac function of the mice was examined (**Figure 1A**). It was found that both the LVEDD and LVESF of mice were elevated. The left ventricular EF and FS were reduced after MI induction. MI led to significant cardiac dysfunction in mice. The TTC staining results indicated significant infarction in model mice (**Figure 1B**). H&E staining suggested that compared to the sham-operated mice, the model mice showed significant cardiomyocyte hypertrophy, inflammatory infiltration, and increased pathological scores in the infarcted border zone (**Figure 1C**). Masson's trichrome staining results showed that the mouse with MI demonstrated significant fibrosis in the infarcted border zone (**Figure 1D**). IHC staining was conducted to examine the level of the apoptosis-related marker c-caspase 3 in the myocardial tissues. It was observed that the c-caspase 3 level was noticeably increased in the infarcted border zone in the myocardium of MI mice (**Figure 1E**). The ELISA results indicated that the IL-6 and TNF-α contents were significantly elevated in the serum of model mice (**Figure 1F**). RT-qPCR and western blot assays showed that SPI1 levels were increased in the infarcted border zone in the myocardium of the mice with MI (**Figure 1G, 1H**). Similar trends were observed by the IHC staining that the positive staining of SPI1 was significantly enhanced in the border zone in the myocardium of MI mice (**Figure 1I**).

SPI1 siRNA reduced hypoxia-induced damage in cardiomyocytes

The HL-1 cells were exposed to a hypoxic condition *in vitro* to mimic cell injury in the infarcted border zone in permanent coronary occlusion-induced MI *in vivo*. Cells cultured in normoxic condition were set as controls. It was observed

SPI1-mediated TLR4 augments cardiac injury in MI



SPI1-mediated TLR4 augments cardiac injury in MI

Figure 1. SPI1 expression was increased in cardiac tissues of model mice. (A) Cardiac function of mice after MI induction or sham operation (n = 10); (B) MI in mice after LAD artery ligation determined by TTC staining (n = 5); (C) Pathological changes in the infarcted border zone in mouse cardiac tissues after MI induction examined by H&E staining (n = 5); (D) Collagen deposition in the infarcted border zone determined by Masson's trichrome staining (n = 5); (E) c-caspase-3 expression in the infarcted border zone in mouse cardiac tissues examined by IHC staining (n = 5); (F) Production of IL-6 and TNF- α in mouse serum examined using ELISA kits (n = 10); (G, H) mRNA (G) and protein (H) levels of SPI1 in the infarcted border zone in mouse cardiac tissues examined by RT-qPCR and western blot analysis (n = 10); (I) SPI1 expression in the infarcted border zone in mouse cardiac tissues examined by IHC staining (n = 5). All data are presented as mean \pm SD. Differences were analyzed by the unpaired *t* test (A-E, G-I) or two-way ANOVA (F). **P* < 0.05 vs. the sham group.

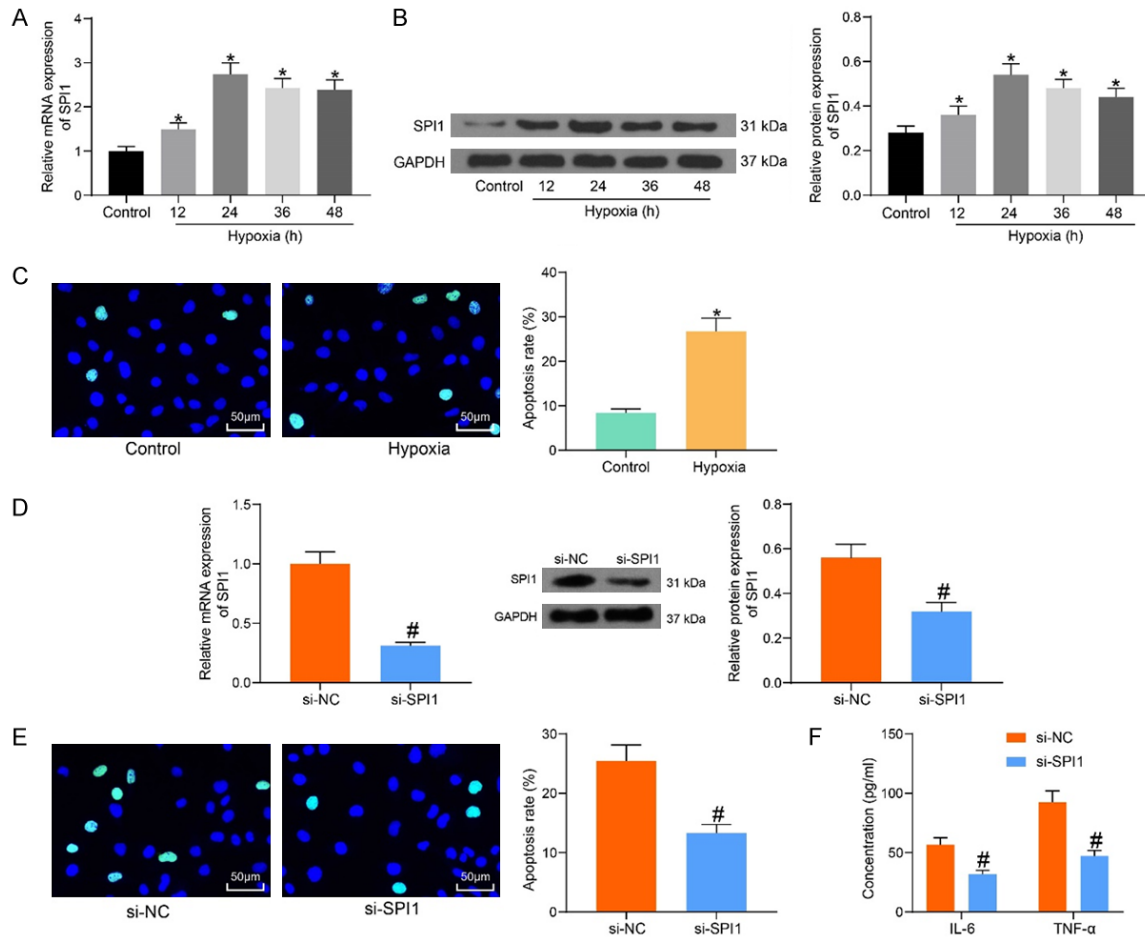


Figure 2. SPI1 siRNA reduced hypoxia-induced damage in cardiomyocytes. (A, B) mRNA (A) and protein (B) levels of SPI1 in HL-1 cells after different time of hypoxic treatment determined by RT-qPCR and western blot analysis; (C) Apoptosis rate in HL-1 cells after hypoxic treatment examined by TUNEL assay; (D) mRNA and protein levels of SPI1 in HL-1 cells after si-SPI1 transfection quantified by RT-qPCR and western blot analysis; (E) Apoptosis rate in HL-1 cells after SPI1 silencing determined by TUNEL assay; (F) Production of IL-6 and TNF- α in the supernatant of SPI1 cells examined using ELISA kits. All data are presented as mean \pm SD. For cellular experiments, repetition = 3. Differences were analyzed by the unpaired *t* test (C-E), one-way ANOVA (A and B) or two-way ANOVA (F). **P* < 0.05 vs. the control group; #*P* < 0.05 vs. the si-NC group.

that the SPI1 levels in HL-1 cells were incrementally increased with the prolongation of hypoxia treatment. The peak value was reached at the 24th h (Figure 2A, 2B). Hypoxic treatment for 24 h was selected as the treating scheme for the subsequent experiments. The

TUNEL assay suggested that the hypoxic treatment promoted the apoptosis rate of HL-1 cells (Figure 2C).

HL-1 cells were transfected with si-SPI1 or si-NC, followed by hypoxic treatment. Successful

SPI1-mediated TLR4 augments cardiac injury in MI

downregulation of SPI1 in cells was detected by RT-qPCR and western blot analysis (**Figure 2D**). The TUNEL assay showed that the cell apoptosis was reduced upon SPI1 inhibition (**Figure 2E**). The production of inflammatory cytokines in the cell supernatant was examined. Pre-transfection of si-SPI1 significantly blocked the release of IL-6 and TNF- α in the hypoxia-induced HL-1 cells (**Figure 2F**).

TLR4 was a potential downstream target of SPI1

We explored the potential downstream targets of SPI1 in cardiomyocytes using the hTF-target system (<http://bioinfo.life.hust.edu.cn/hTFtarget/#/>). The top 100 candidate targets were collected for pathway enrichment analyses (**Figure 3A**). Genes enriched in the inflammation- and apoptosis-related pathways were screened for further analysis (**Figure 3B**). TLR4 was identified to be intersected (**Figure 3C**).

The expression of TLR4 in the model mice was examined. In the infarcted border zone in myocardium, the TLR4 levels were significantly elevated after MI induction (**Figure 3D, 3E**). *In vitro*, the TLR4 expression in HL-1 cells was increased after hypoxic treatment. The upregulation of TLR4 in hypoxia-treated cells was blocked by pre-transfection of si-SPI1 in cells (**Figure 3F, 3G**).

SPI1 bound to the TLR4 promoter for transcriptional activation

The information of TLR4 was obtained from the hTFtarget system (**Figure 4A**). According to the ChIP-seq using the Cistrome Data Browser (<http://cistrome.org/db/#/>), there was a significant binding peak between SPI1 and TLR4 promoter in the mouse genome (**Figure 4B**). The candidate binding sites were predicted using the Jaspas system. The site with the highest predictive score (**Figure 4C**) was used for a ChIP-qPCR assay. An abundance of TLR4 promoter sequences was enriched by anti-SPI1 compared to IgG (**Figure 4D**). The dual-luciferase reporter assay suggested that downregulation of SPI1 significantly suppressed the transcriptional activity of TLR4 Promoter-WT but did not influence the transcriptional activity of the TLR4 Promoter-MT in HL-1 cells (**Figure 4E**).

Overexpression of TLR4 activated the NF κ B signaling pathway and blocked the protective roles of SPI1 siRNA

TLR4 has been reported to mediate NF κ B phosphorylation to augment myocardial injury in MI [16]. To validate this, the TLR4 overexpressing vector oe-TLR4 and the control vector oe-NC were administrated into HL-1 cells after si-SPI1 transfection. The SPI1 and TLR4 levels and the NF κ B activity in cells were determined by western blot analysis (**Figure 5A**). It was found that the SPI1 and TLR4 levels and the NF κ B phosphorylation in cells were significantly reduced by si-SPI1. The oe-TLR4 did not affect the level of SPI1, but it restored the TLR4 protein level and the phosphorylation of NF κ B suppressed by si-SPI1.

The apoptosis and inflammation in cells were examined. The TUNEL assay suggested that overexpression of TLR4 enhanced the apoptosis of HL-1 cells suppressed by si-SPI1 (**Figure 5B**). The ELISA results suggested that the IL-6 and TNF- α levels in the cell supernatant was increased by oe-TLR4 (**Figure 5C**).

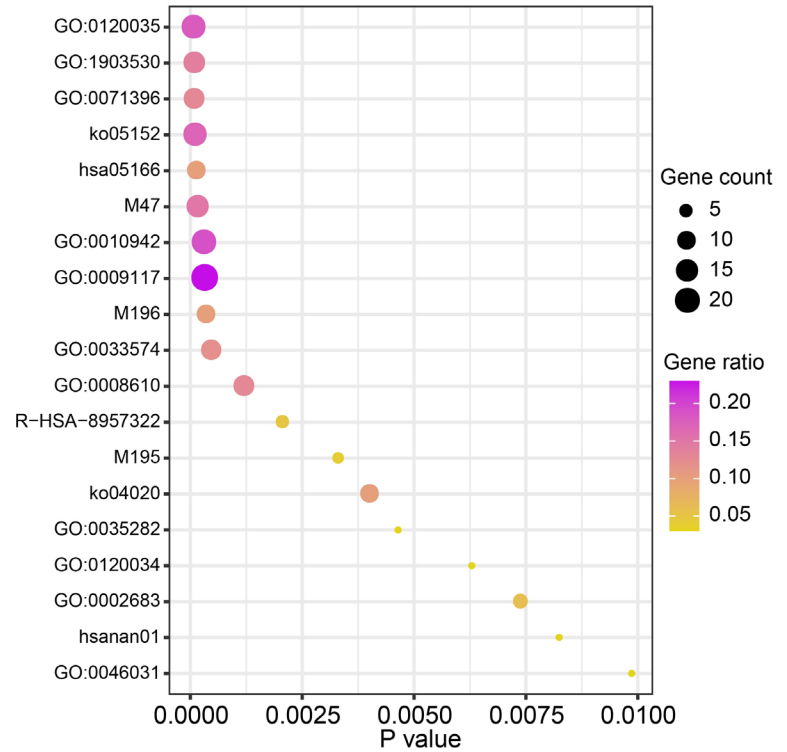
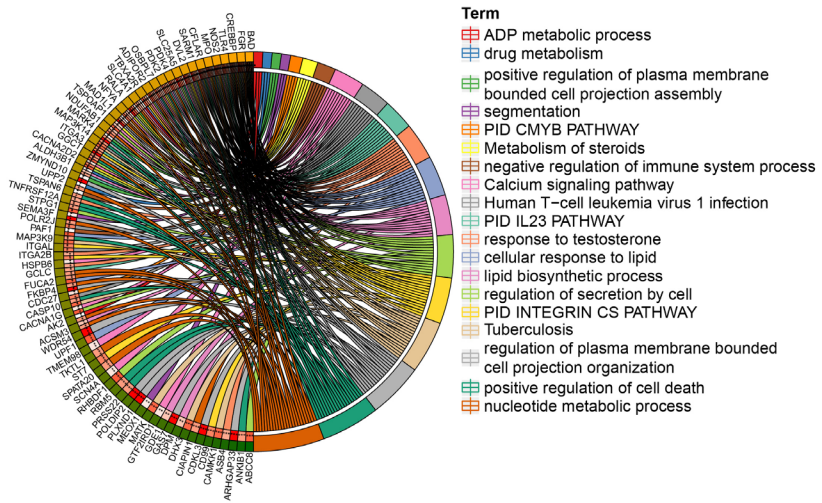
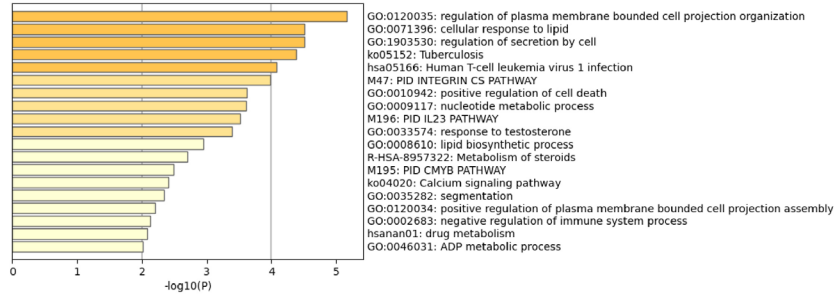
Another group of HL-1 cells were transfected with oe-TLR4 only, followed by hypoxic exposure. It was found that the TLR4 treatment significantly aggravated the phosphorylation of NF κ B in cells (**Figure 5D**) and increased cell apoptosis (**Figure 5E**) and the production of inflammatory cytokines (**Figure 5F**).

Silencing of SPI1 inhibited the TLR4/NF κ B axis and reduced injury in mice with MI

The correlation between SPI1 and the TLR4/NF κ B axis was validated *in vivo*. AAV-siRNA-SPI1 and AAV-TLR4 and the corresponding controls were injected into the cardiac tissues of mice one week before MI induction. The LVEDD and LVESD of mice were reduced. The left ventricular EF and FS were increased in mice pre-injected with AAV-siRNA-SPI1 relative to those pre-injected with AAV-NC. The cardiac function of mice was reduced after more administration of AAV-TLR4 (**Figure 6A**). The IHC staining showed that the SPI1, TLR4, p-NF κ B, and c-caspase 3 levels in the infarcted border zone in the myocardium of mice were

SPI1-mediated TLR4 augments cardiac injury in MI

A



SPI1-mediated TLR4 augments cardiac injury in MI

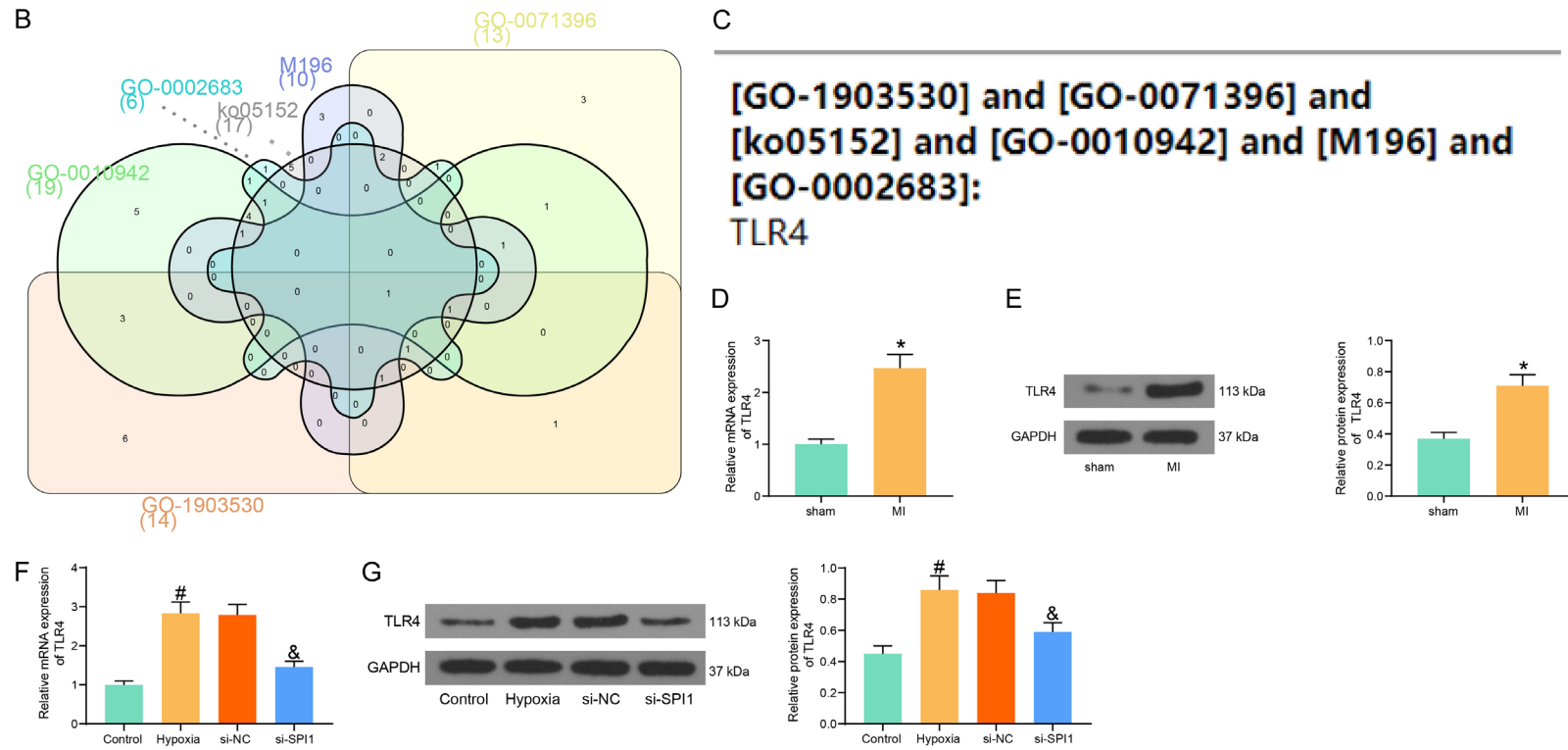


Figure 3. TLR4 was a potential downstream target of SPI1. (A) Pathway enrichment analyses of the candidate downstream genes of SPI1; (B) Downstream genes of SPI1 enriched in the inflammation- and apoptosis-related signaling pathways; (C) The intersected gene in several related signaling pathways; (D, E) mRNA (D) and protein (E) levels of TLR4 in infarcted border zone in cardiac tissues of model mice and sham-operated ones detected by RT-qPCR and western blot analysis (n = 10); (F, G) mRNA (F) and protein (G) levels of TLR4 in hypoxia-treated HL-1 cells evaluated by RT-qPCR and western blot analysis. All data are presented as mean ± SD. For cellular experiments, repetition = 3. Differences were analyzed by the unpaired *t* test (D and E) or one-way ANOVA (F and G). **P* < 0.05 vs. the sham group; #*P* < 0.05 vs. the control group (normoxic condition); &*P* < 0.05 vs. the si-NC group.

SPI1-mediated TLR4 augments cardiac injury in MI

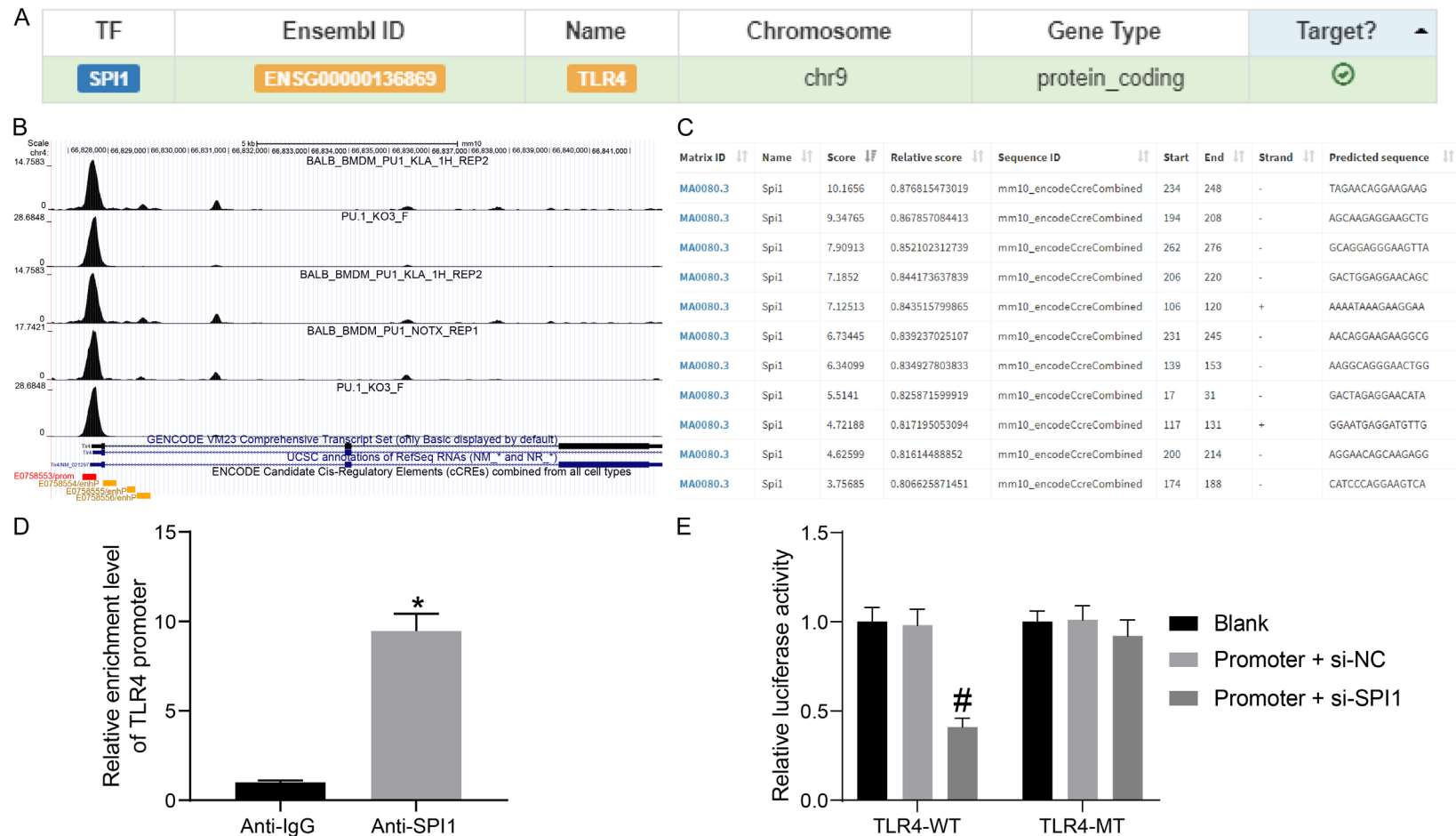


Figure 4. SPI1 bound to the TLR4 promoter for transcriptional activation. (A) TLR4 as target transcript of SPI1 predicted in the hTFtarget system; (B) A binding peak between SPI1 and TLR4 promoter in the mouse genome according to the ChIP-seq analysis; (C) Binding sites of SPI1 to TLR4 promoter predicted from the Jaspar system; (D) Enrichment of TLR4 promoter fragments by anti-SPI1 examined using the ChIP-qPCR assay; (E) Binding between SPI1 and TLR4 promoter validated by luciferase reporter assay. All data are presented as mean \pm SD. For cellular experiments, repetition = 3. Differences were analyzed by the unpaired *t* test (D) or two-way ANOVA (E). **P* < 0.05 vs. anti-IgG; #*P* < 0.05 vs. the Promoter + si-NC group.

SPI1-mediated TLR4 augments cardiac injury in MI

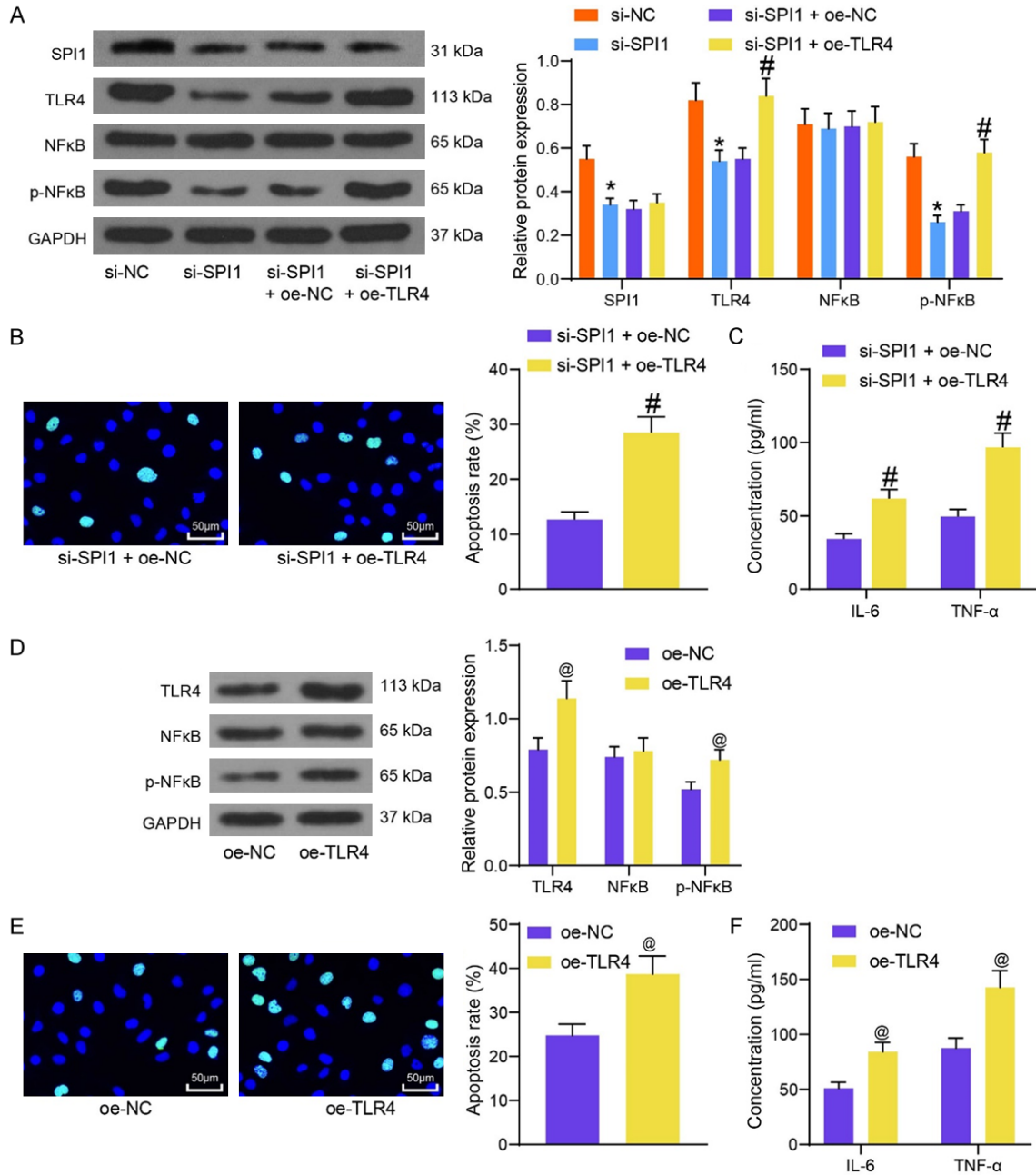
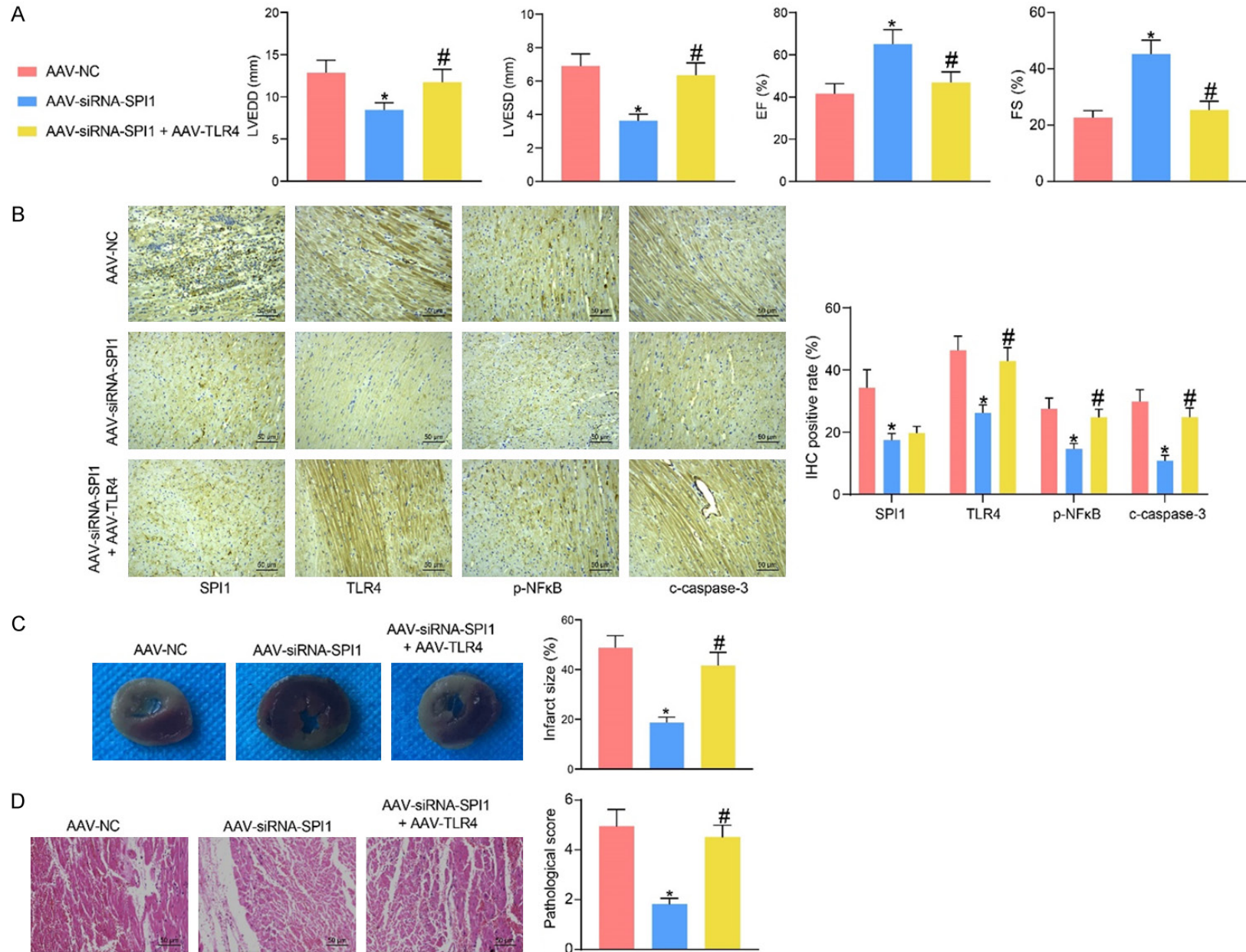


Figure 5. Overexpression of TLR4 activated the NFκB signaling pathway and blocked the protective roles of SPI1 siRNA. (A) SPI1 and TLR4 protein levels and the NFκB phosphorylation in HL-1 cells after si-SPI1 and oe-TLR4 transfection and hypoxia exposure determined using western blot analysis; (B) Apoptosis of HL-1 cells examined by the TUNEL assay; (C) Secretion of IL-6 and TNF-α in cells examined using ELISA kits; (D) Protein level of TLR4 and phosphorylation of NFκB in HL-1 cells after oe-TLR4 transfection and hypoxia exposure determined using western blot analysis; (E) Cell apoptosis examined by the TUNEL assay; (F) Secretion of the pro-inflammatory cytokines in cells examined using ELISA kits. For cellular experiments, repetition = 3. All data are presented as mean ± SD. Differences were analyzed by the unpaired *t* test (B and E) or two-way ANOVA (A, C, D, and F). **P* < 0.05 vs. oe-NC; #*P* < 0.05 vs. the si-SPI1 + oe-NC group; @*P* < 0.05 vs. oe-NC.

reduced by AAV-siRNA-SPI1 but rescued by AAV-TLR4 (Figure 6B). The TTC staining suggested that the myocardial injury in the cardiac tissues of mice was reduced by the pre-injec-

tion of AAV-siRNA-SPI1 but aggravated by the pre-injection of AAV-TLR4 in mice (Figure 6C). The H&E staining suggested that the inflammatory infiltration and cardiomyocyte hypertro-

SPI1-mediated TLR4 augments cardiac injury in MI



SPI1-mediated TLR4 augments cardiac injury in MI

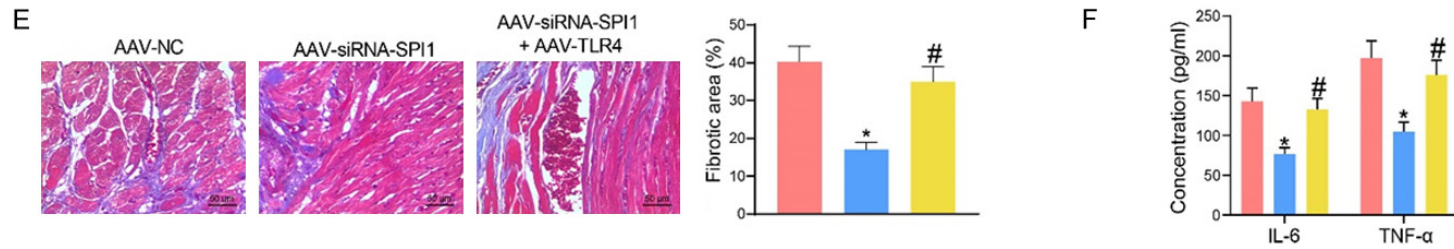
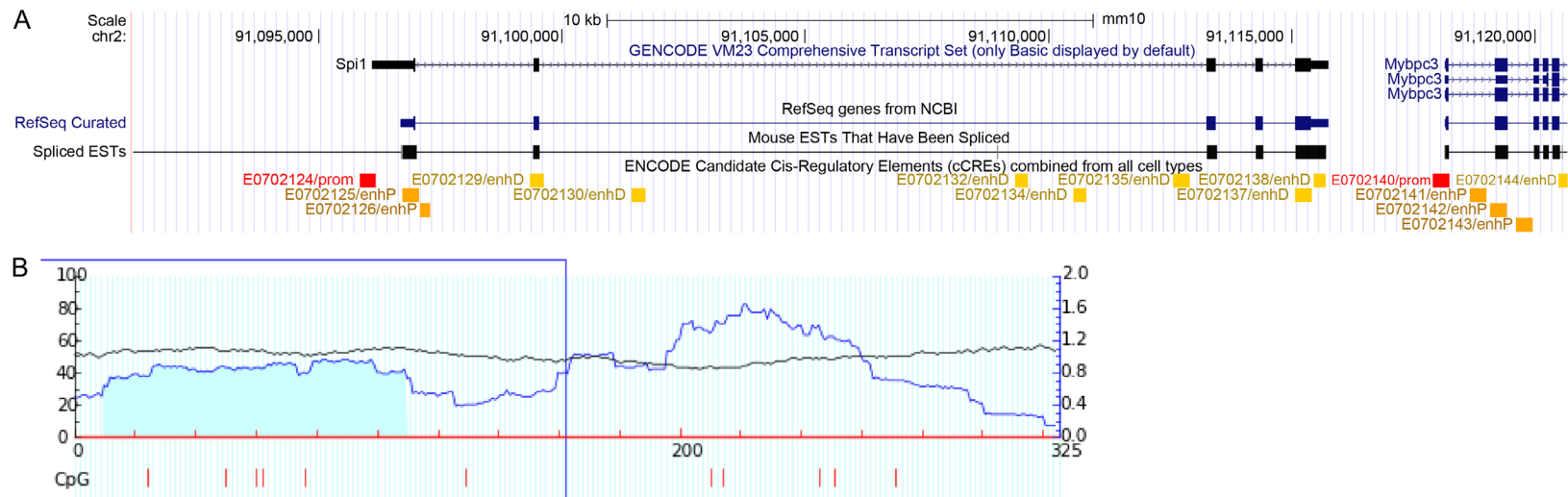


Figure 6. Silencing of SPI1 inhibited the TLR4/NFκB axis and reduced injury in mice with MI. (A) Cardiac function of mice after AAV administration and MI induction (n = 10); (B) Levels of SPI1, TLR4, p-NFκB, and c-caspase 3 in infarcted border zone in mouse cardiac tissues examined by IHC staining (n = 5); (C) Myocardial injury in mice determined by TTC staining (n = 5); (D) Pathological changes in mouse cardiac tissues examined by H&E staining (n = 5); (E) Collagen deposition in mouse cardiac tissues determined by Masson's trichrome staining (n = 5); (F) Secretion of pro-IL-6 and TNF-α in mouse serum examined using ELISA kits (n = 10). All data are presented as mean ± SD. Differences were analyzed by one-way (A, C, and E) or two-way (B and F) ANOVA. *P < 0.05 vs. the AAV-NC group; #P < 0.05 vs. the AAV-siRNA-SPI1 group.



SPI1-mediated TLR4 augments cardiac injury in MI

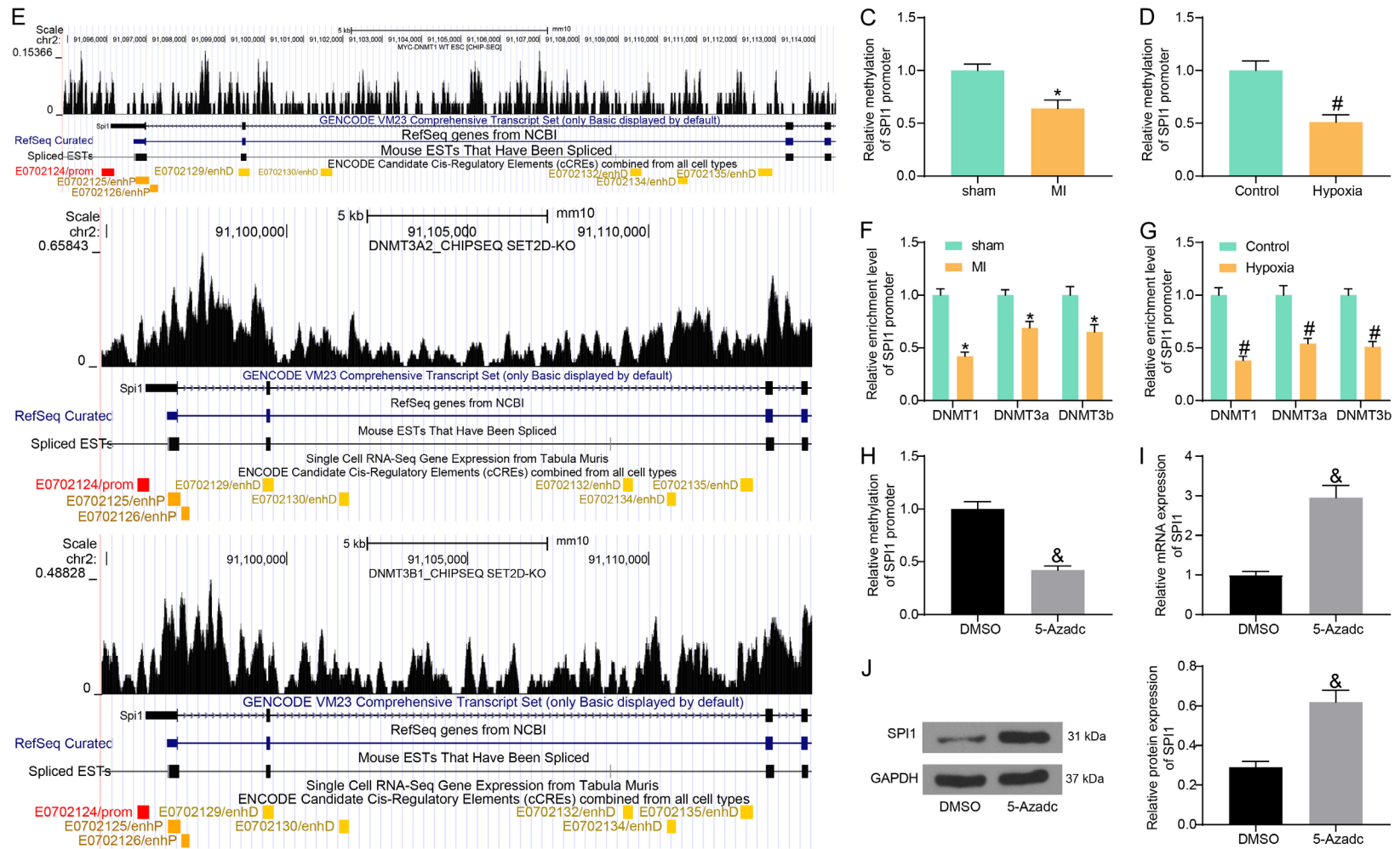


Figure 7. High expression of SPI1 in MI was attributed to low level of DNA methylation. (A) Location of SPI1 promoter in mouse genome; (B) CpG island on the SPI1 promoter; (C, D) DNA methylation level of SPI1 in mouse cardiac tissues (C) and in HL-1 cells (D) examined by qMSP; (E) Binding peaks between DNMTs with SPI1 promoter according to the ChIP-seq analysis; (F, G) Abundance of DNMTs in the promoter region of SPI1 in mouse cardiac tissues (F) and HL-1 cells (G) examined by ChIP-qPCR; (H) DNA methylation in SPI1 promoter in HL-1 cells after 5-Azadc treatment examined by qMSP; (I, J) mRNA (I) and protein (J) levels of SPI1 in HL-1 cells after 5-Azadc treatment determined by RT-qPCR and western blot analysis. For cellular experiments, repetition = 3. All data are presented as mean \pm SD. Differences were analyzed by unpaired t test (C, D, H, and I) or two-way ANOVA (F and G). *P < 0.05 vs. the sham group; #P < 0.05 vs. the control group; &P < 0.05 vs. the DMSO group.

SPI1-mediated TLR4 augments cardiac injury in MI

phy in the infarcted border zone was suppressed by the downregulation of SPI1, but this suppression was blocked after TLR4 overexpression (**Figure 6D**). The Masson's trichrome staining revealed that downregulation of SPI1 reduced the overall infarct size in the myocardium and the myocardial fibrosis in the border zone. The protective function of SPI1 inhibition against fibrosis was blocked again by TLR4 overexpression (**Figure 6E**). The ELISA results indicated that the IL-6 and TNF- α levels in mouse serum were reduced by SPI1 silencing but increased by TLR4 restoration (**Figure 6F**). These results indicated that silencing of SPI1 inactivated the TLR4/NF κ B axis and reduced injury in mice with MI.

High expression of SPI1 in MI was attributed to low level of DNA methylation

The transcriptional activity of SPI1 has been associated with the DNA methylation level [17, 18]. To examine this, we obtained the promoter sequence of SPI1 from the UCSC system (<https://genome.ucsc.edu/index.html>) (**Figure 7A**). The CpG island on the SPI1 promoter was analyzed using Methprimer2 (<http://www.uro-gene.org/methprimer2/tester-invitation.html>) (**Figure 7B**). The qMSP results suggested that the DNA methylation in the CpG island on the SPI1 promoter was significantly reduced in mice with MI and in hypoxia-treated HL-1 cells (**Figure 7C, 7D**). The ChIP-seq analysis suggested that several DNMTs including DNMT1, DNMT3a, and DNMT3b have binding peaks with the SPI1 promoter (**Figure 7E**). The ChIP-qPCR assay showed that the abundance of the DNMTs in the CpG island on the SPI1 promoter was reduced in mice with MI and in hypoxia-treated HL-1 cells (**Figure 7F, 7G**). The HL-1 cells were treated with a DNMT-specific inhibitor 5-Azadc. The qMSP results indicated that the DNA methylation of SPI1 was significantly reduced after by 5-Azadc (**Figure 7H**). The SPI1 levels in cells was upregulated after 5-Azadc treatment (**Figure 7I, 7J**).

Discussion

The ischemic heart disease following MI remains a health issue that leads to disability and mortality worldwide [19]. An immediate in-hospital therapy is of primary importance for MI treatment [1]. Secondary reperfusion injury may occur after the operation and thromboly-

sis, which contributes to more irreversible cardiomyocyte death [20]. Myocardial apoptosis, inflammation, and fibrosis are key events during MI. Identifying key molecules involved in these events may help develop novel strategies for MI management. This study confirmed that reduced DNA methylation-induced upregulation of SPI1 augmented cardiac injury during MI by activating the TLR4/NF κ B axis.

SPI1 has been implicated in the development of post-MI heart failure and correlated with inflammation, immune activity, and cell apoptosis [8]. To probe the function of SPI1 in MI, we examined the SPI1 expression in MI models. SPI1 was significantly upregulated in model mice and in hypoxia-induced HL-1 cells. In a recent publication by Gang *et al.*, SPI1 mRNA was upregulated and correlated with the transcription activation of interleukin (IL)-9 and Th9 cell activation in patients with acute MI [21]. SPI1 expression has been upregulated in hypoxic endothelium by RUNX family transcription factor 1 and CEBP α [22]. SPI1 has been identified as a transcriptional factor upregulated in a murine model with cerebral ischemia-reperfusion injury, and it combined with CEBP α to promote the activity of monocyte-specific promoter and affect NF κ B activity [23, 24], indicating its potential role in inflammatory responses. We found siRNA silencing of SPI1 significantly reduced hypoxia-induced apoptosis, release of IL-6 and TNF- α , and the levels of fibrosis-related α -SMA and COL1A1 in cells. SPI1 inhibition restored cardiac function and alleviated myocardial inflammation and fibrosis in mouse cardiac tissues. The pro-inflammatory role of SPI1 has been observed in asthmatic airway inflammation [25] and in microglial-induced inflammation in secondary spinal cord injury [26]. SPI1 has been reported as a critical regulator of the pro-fibrotic gene expression program whose activation induces fibrosis-associated genes and pro-fibrotic fibroblasts [27]. We found that SPI1 upregulation played potent pro-apoptotic, pro-fibrotic, and pro-inflammatory, and roles in cardiac tissues and cells during MI.

With the aid of advanced bioinformatic tools and analytic methods, TLR4 was identified as a downstream target of SPI1. The binding of SPI1 with TLR4 promoter was validated by ChIP-qPCR and luciferase reporter assays. We identified increased expression of TLR4 in the

SPI1-mediated TLR4 augments cardiac injury in MI

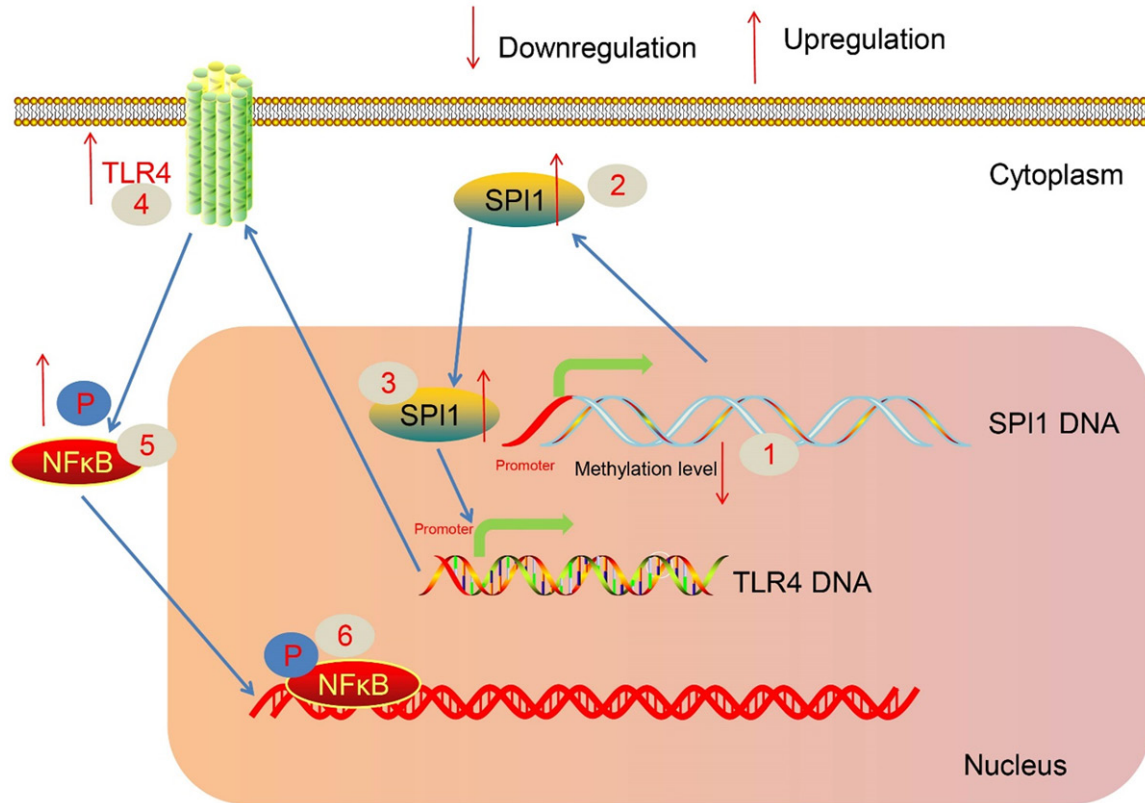


Figure 8. Diagram presentation for the molecules of action. During MI, the DNA methylation of SPI1 is significantly reduced, which leads to SPI1 transcriptional activation. SPI1 binds to the TLR4 promoter and promotes TLR4 transcription, which augments inflammatory responses and myocardial fibrosis by inducing NFκB phosphorylation.

tissues of model mice with MI and in hypoxia-treated cardiomyocytes. TLR4 activates a variety of transcriptional factors including NFκB, which is a master regulator of inflammation and is responsible for the production of the pro-inflammatory cytokines [10, 28]. The TLR4/NFκB activation has been frequently involved in the pathogenesis of MI and induced tissue injury and inflammation [29, 30]. Inhibition of the TLR4/NFκB has been demonstrated as a promising target for the anti-apoptotic and anti-inflammatory managements for MI [13, 31-33]. In this study, we found that silencing of SPI1 decreased the TLR4 expression and NFκB phosphorylation in the hypoxia-treated HL-1 cells and the tissues of model mice. Artificial overexpression of TLR4 restored NFκB phosphorylation and rescued the production of inflammatory and fibrosis-related factors, indicating that the TLR4/NFκB activation was responsible for the aggravating roles of SPI1 in MI.

The transcriptional activity of SPI1 has been associated with the level of DNA methylation, a

classic manner of epigenetic regulation [17, 18]. DNA methylation suppresses gene transcription by recruiting proteins responsible for gene repression or blocking the binding of transcription factor(s) to DNA [34]. We examined the DNA methylation level of SPI1 in the animal and cell models. We confirmed significant binding peaks between the SPI1 promoter and DNMTs. The DNA methylation level in the CpG island on the SPI1 promoter was significantly reduced in mice with MI and in hypoxia-exposed HL-1 cells, which led to elevated expression of SPI1.

This work demonstrates that during the disease course of MI, the DNA methylation of SPI1 is significantly reduced, which leads to SPI1 transcriptional activation. Upregulated SPI1 binds to the TLR4 promoter and activates the TLR4/NFκB axis, which aggravates myocardial apoptosis, inflammation, and fibrosis in cardiac tissues (**Figure 8**). Although mechanism for the aberrant DNA methylation of SPI1 promoter remains unelucidated in the study, this work may provide new understanding in

the management of MI that SPI1 may serve as a biomarker or treating target for the treatment of MI. To avoid unnecessary animal death and because of time and funding limitations, we detected parameters such as the cardiac function, inflammation, and cell apoptosis at the same time point for the *in vivo* experiments (the 14th day after MI induction). It might be more appropriate to analyze these parameters at different time points to obtain more representative and integrate results. We would like to include more animal samples to validate the SPI1/TLR4/NFκB axis in MI in the near future.

Disclosure of conflict of interest

None.

Address correspondence to: Shuai Huang, Department of Cardiovascular Medicine, Panjin Liaohe Oil Gem Flower Hospital, No. 23, Liaohe Middle Road, Xinglongtai District, Panjin 124010, Liaoning, P. R. China. Tel: +86-15804108584; Fax: +86-15804108584; E-mail: huangshuai1291@126.com

References

- [1] Lu L, Liu M, Sun R, Zheng Y and Zhang P. Myocardial infarction: symptoms and treatments. *Cell Biochem Biophys* 2015; 72: 865-867.
- [2] Kosuge M, Kimura K, Ishikawa T, Ebina T, Hibi K, Tsukahara K, Kanna M, Iwahashi N, Okuda J, Nozawa N, Ozaki H, Yano H, Nakati T, Kusama I and Umemura S. Differences between men and women in terms of clinical features of ST-segment elevation acute myocardial infarction. *Circ J* 2006; 70: 222-226.
- [3] Saleh M and Ambrose JA. Understanding myocardial infarction. *F1000Res* 2018; 7: F1000.
- [4] Bejerano T, Etzion S, Elyagon S, Etzion Y and Cohen S. Nanoparticle delivery of miRNA-21 mimic to cardiac macrophages improves myocardial remodeling after myocardial infarction. *Nano Lett* 2018; 18: 5885-5891.
- [5] Wang Y, Ju C, Hu J, Huang K and Yang L. PRMT4 overexpression aggravates cardiac remodeling following myocardial infarction by promoting cardiomyocyte apoptosis. *Biochem Biophys Res Commun* 2019; 520: 645-650.
- [6] Roos-Weil D, Decaudin C, Armand M, Della-Valle V, Diop MK, Ghamlouch H, Ropars V, Herate C, Lara D, Durot E, Haddad R, Mylonas E, Damm F, Pflumio F, Stoilova B, Metzner M, Elemento O, Dessen P, Camara-Clayette V, Cosset FL, Verhoeven E, Leblond V, Ribrag V, Cornillet-Lefebvre P, Rameau P, Azar N, Charlotte F, Morel P, Charbonnier JB, Vyas P, Mercher T, Aoufouchi S, Droin N, Guillouf C, Nguyen-Khac F and Bernard OA. A recurrent activating missense mutation in waldenstrom macroglobulinemia affects the DNA binding of the ETS transcription factor SPI1 and enhances proliferation. *Cancer Discov* 2019; 9: 796-811.
- [7] Huang KL, Marcora E, Pimenova AA, Di Narzo AF, Kapoor M, Jin SC, Harari O, Bertelsen S, Fairfax BP, Czajkowski J, Chouraki V, Grenier-Boley B, Bellenguez C, Deming Y, McKenzie A, Raj T, Renton AE, Budde J, Smith A, Fitzpatrick A, Bis JC, DeStefano A, Adams HHH, Ikram MA, van der Lee S, Del-Aguila JL, Fernandez MV, Ibañez L; International Genomics of Alzheimer's Project; Alzheimer's Disease Neuroimaging Initiative, Sims R, Escott-Price V, Mayeux R, Haines JL, Farrer LA, Pericak-Vance MA, Lambert JC, van Duijn C, Launer L, Seshadri S, Williams J, Amouyel P, Schellenberg GD, Zhang B, Borecki I, Kauwe JSK, Cruchaga C, Hao K and Goate AM. A common haplotype lowers PU.1 expression in myeloid cells and delays onset of Alzheimer's disease. *Nat Neurosci* 2017; 20: 1052-1061.
- [8] Niu X, Zhang J, Zhang L, Hou Y, Pu S, Chu A, Bai M and Zhang Z. Weighted gene co-expression network analysis identifies critical genes in the development of heart failure after acute myocardial infarction. *Front Genet* 2019; 10: 1214.
- [9] Ramirez-Carracedo R, Tesoro L, Hernandez I, Diez-Mata J, Pineiro D, Hernandez-Jimenez M, Zamorano JL and Zaragoza C. Targeting TLR4 with ApTOLL improves heart function in response to coronary ischemia reperfusion in pigs undergoing acute myocardial infarction. *Biomolecules* 2020; 10: 1167.
- [10] Yang Y, Lv J, Jiang S, Ma Z, Wang D, Hu W, Deng C, Fan C, Di S, Sun Y and Yi W. The emerging role of Toll-like receptor 4 in myocardial inflammation. *Cell Death Dis* 2016; 7: e2234.
- [11] Yan ZQ. Regulation of TLR4 expression is a tale about tail. *Arterioscler Thromb Vasc Biol* 2006; 26: 2582-2584.
- [12] Bhattacharya D and Yusuf N. Expression of toll-like receptors on breast tumors: taking a toll on tumor microenvironment. *Int J Breast Cancer* 2012; 2012: 716564.
- [13] Wang XZ, Yu ZX, Nie B and Chen DM. Perindopril inhibits myocardial apoptosis in mice with acute myocardial infarction through TLR4/NF-kappaB pathway. *Eur Rev Med Pharmacol Sci* 2019; 23: 6672-6682.
- [14] Liu D, Tian X, Liu Y, Song H, Cheng X, Zhang X, Yan C and Han Y. CREG ameliorates the phenotypic switching of cardiac fibroblasts after myocardial infarction via modulation of CDC42. *Cell Death Dis* 2021; 12: 355.
- [15] Wei Z, Fei Y, Wang Q, Hou J, Cai X, Yang Y, Chen T, Xu Q, Wang Y and Li YG. Loss of Camk2n1 aggravates cardiac remodeling and malignant

SPI1-mediated TLR4 augments cardiac injury in MI

- ventricular arrhythmia after myocardial infarction in mice via NLRP3 inflammasome activation. *Free Radic Biol Med* 2021; 167: 243-257.
- [16] Yu P, Li Y, Fu W, Li X, Liu Y, Wang Y, Yu X, Xu H and Sui D. Panax quinquefolius L. Saponins protect myocardial ischemia reperfusion no-reflow through inhibiting the activation of NLRP3 inflammasome via TLR4/MyD88/NF-kappaB signaling pathway. *Front Pharmacol* 2020; 11: 607813.
- [17] Özdemir İ, Pınarlı FG, Pınarlı FA, Aksakal FNB, Okur A, Uyar Gökün P and Karadeniz C. Epigenetic silencing of the tumor suppressor genes SPI1, PRDX2, KLF4, DLEC1, and DAPK1 in childhood and adolescent lymphomas. *Pediatr Hematol Oncol* 2018; 35: 131-144.
- [18] Marthong L, Ghosh S, Palodhi A, Imran M, Shunyu NB, Maitra A and Ghosh S. Whole genome DNA methylation and gene expression profiling of oropharyngeal cancer patients in North-Eastern India: identification of epigenetically altered gene expression reveals potential biomarkers. *Front Genet* 2020; 11: 986.
- [19] Wu J, Hall M, Dondo TB, Wilkinson C, Ludman P, DeBelder M, Fox KAA, Timmis A and Gale CP. Association between time of hospitalization with acute myocardial infarction and in-hospital mortality. *Eur Heart J* 2019; 40: 1214-1221.
- [20] Song Y, Zhang C, Zhang J, Jiao Z, Dong N, Wang G, Wang Z and Wang L. Localized injection of miRNA-21-enriched extracellular vesicles effectively restores cardiac function after myocardial infarction. *Theranostics* 2019; 9: 2346-2360.
- [21] Gang H, Peng D, Hu Y, Tang S, Li S and Huang Q. Interleukin-9-secreting CD4(+) T cells regulate CD8(+) T cells cytotoxicity in patients with acute coronary syndromes. *APMIS* 2021; 129: 91-102.
- [22] Ghosh G, Subramanian IV, Adhikari N, Zhang X, Joshi HP, Basi D, Chandrashekhhar YS, Hall JL, Roy S, Zeng Y and Ramakrishnan S. Hypoxia-induced microRNA-424 expression in human endothelial cells regulates HIF-alpha isoforms and promotes angiogenesis. *J Clin Invest* 2010; 120: 4141-4154.
- [23] Jin F, Li Y, Ren B and Natarajan R. PU.1 and C/EBP(alpha) synergistically program distinct response to NF-kappaB activation through establishing monocyte specific enhancers. *Proc Natl Acad Sci U S A* 2011; 108: 5290-5295.
- [24] Zhang YY, Wang K, Liu YE, Wang W, Liu AF, Zhou J, Li C, Zhang YQ, Zhang AP, Lv J and Jiang WJ. Identification of key transcription factors associated with cerebral ischemiareperfusion injury based on geneset enrichment analysis. *Int J Mol Med* 2019; 43: 2429-2439.
- [25] Qian F, Deng J, Lee YG, Zhu J, Karpurapu M, Chung S, Zheng JN, Xiao L, Park GY and Christman JW. The transcription factor PU.1 promotes alternative macrophage polarization and asthmatic airway inflammation. *J Mol Cell Biol* 2015; 7: 557-567.
- [26] Yu M, Ou Y, Wang H and Gu W. PU.1 interaction with p50 promotes microglial-mediated inflammation in secondary spinal cord injury in SCI rats. *Int J Neurosci* 2021; 1-15.
- [27] Wohlfahrt T, Rauber S, Uebe S, Lubert M, Soare A, Ekici A, Weber S, Matei AE, Chen CW, Maier C, Karouzakis E, Kiener HP, Pachera E, Dees C, Beyer C, Daniel C, Gelse K, Kremer AE, Naschberger E, Sturzl M, Butter F, Sticherling M, Finotto S, Kreuter A, Kaplan MH, Jungel A, Gay S, Nutt SL, Boykin DW, Poon GMK, Distler O, Schett G, Distler JHW and Ramming A. PU.1 controls fibroblast polarization and tissue fibrosis. *Nature* 2019; 566: 344-349.
- [28] Jiang Q, Yi M, Guo Q, Wang C, Wang H, Meng S, Liu C, Fu Y, Ji H and Chen T. Protective effects of polydatin on lipopolysaccharide-induced acute lung injury through TLR4-MyD88-NF-kappaB pathway. *Int Immunopharmacol* 2015; 29: 370-376.
- [29] Li Y, Wang J, Sun L and Zhu S. LncRNA myocardial infarction-associated transcript (MIAT) contributed to cardiac hypertrophy by regulating TLR4 via miR-93. *Eur J Pharmacol* 2018; 818: 508-517.
- [30] Liu M, Yin L, Li W, Hu J, Wang H, Ye B, Tang Y and Huang C. C1q/TNF-related protein-9 promotes macrophage polarization and improves cardiac dysfunction after myocardial infarction. *J Cell Physiol* 2019; 234: 18731-18747.
- [31] Ma C, Jiang Y, Zhang X, Chen X, Liu Z and Tian X. Isoquercetin ameliorates myocardial infarction through anti-inflammation and anti-apoptosis factor and regulating TLR4-NF-kappaB signal pathway. *Mol Med Rep* 2018; 17: 6675-6680.
- [32] Li H, Yang H, Wang D, Zhang L and Ma T. Peroxiredoxin2 (Prdx2) reduces oxidative stress and apoptosis of myocardial cells induced by acute myocardial infarction by inhibiting the TLR4/Nuclear Factor kappa B (NF-kappaB) signaling pathway. *Med Sci Monit* 2020; 26: e926281.
- [33] Ma H, Du J, Feng X, Zhang Y, Wang H, Ding S, Huang A and Ma J. Rosiglitazone alleviates myocardial apoptosis in rats with acute myocardial infarction via inhibiting TLR4/NF-kappaB signaling pathway. *Exp Ther Med* 2020; 19: 2491-2496.
- [34] Moore LD, Le T and Fan G. DNA methylation and its basic function. *Neuropsychopharmacology* 2013; 38: 23-38.